Publication Year	2018
Acceptance in OA@INAF	2020-11-13T15:27:33Z
Title	Simulating the optical performances of the ATHENA x-ray telescope optics
Authors	SIRONI, GIORGIA; SPIGA, Daniele; Della Monica Ferreira, Desiree; Ferreira, Ivo; Bavdaz, Marcos; et al.
DOI	10.1117/12.2315019
Handle	http://hdl.handle.net/20.500.12386/28336
Series	PROCEEDINGS OF SPIE
Number	10699

Simulating the optical performances of the ATHENA X-ray telescope optics

G. Sironi,[a] D. Della Monica Ferreira,[b] D. Spiga,[a,c] E. Bergbäck Knudsen,[b] M. Bavdaz,[d] G. Bianucci,[e] F. E. Christensen,[b] I. Ferreira,[d] V. Fioretti,[f] A. S Jegers,[b] S. Lotti,[h] C. Macculi,[h] F. Marioni,[e] S. Massahi,[b] S. Molendi,[g] A. Moretti,[a] G. Pareschi,[a] B. Shortt,[d] G. Tagliaferri,[a] G. Valsecchi,[e] N.J. Westergaard,[b] E. Wille,[d]

[a]INAF - Brera Astronomical Observatory, Via Bianchi 46, 23807 Merate, Italy
[b]DTU Space, Techn. Univ. of Denmark, Elektrovej b. 327, 2800 Kgs. Lyngby, Denmark
[c]SLAC National Accelerator Laboratory, 2575 Sand Hill Road, 94025 Menlo Park, USA
[d]European Space Agency, ESTEC, Keplerlaan 1, 2201 AZ Noordwjik, The Netherlands
[e]Media Lario s.r.l., loc. Pascolo, 23842 Bosisio Parini, Italy
[f]INAF - IASF Bologna, Via Gobetti 101, 40129 Bologna, Italy
[g]INAF - IASF Milano, Via Bassini 15, 20133 Milano, Italy
[h]INAF - IAPS, Via Fosso del Cavaliere 100, 00133 Roma, Italy

ABSTRACT

The ATHENA (Advanced Telescope for High Energy Astrophysics) X-ray observatory is an ESA-selected L2 class mission. In the proposed configuration, the optical assembly has a diameter of 2.2 m with an effective area of 1.4 m^2 at 1 keV, 0.25 m^2 at 6 keV and requires an angular resolution of 5 arcsec. To meet the requirements of effective area and angular resolution, the technology of Silicon Pore Optics (SPO) was selected for the optics implementation. The ATHENA's optic assembly requires hundreds of SPOs mirror modules (MMs), obtained by stacking wedged and ribbed silicon wafer plates onto silicon mandrels to form the Wolter-I configuration. Different factors can contribute to limit the imaging performances of SPOs, such as i) diffraction through the pore apertures, ii) plate deformations due to fabrication errors and surface roughness, iii) alignment errors among plates in an MM, and iv) co-focality errors within the MMs assembly. In order to determine the fabrication and assembling tolerances, the impact of these contributions needs to be assessed prior to manufacturing. A complete set of simulation tools responding to this need was developed in the framework of the ESA-financed projects SIMPOSIuM, ASPHEA, and SPIRIT. In this paper, we present the performance simulation obtained for the new proposed ATHENA configuration in terms of effective area and point spread function, and we provide a simulation of the diffractive effects in a pair of SPO MMs. Finally, we present an updated sizing of magnetic diverter (a Halbach array) for charged particle deflection, and the magnetic fields levels that can be reached.

Keywords: ATHENA, Silicon Pore Optics, optical design, simulation, alignment, diffraction

1. INTRODUCTION

The ATHENA X-ray observatory,[1] is an ESA large mission selected in the Cosmic Vision plan. The mission is planned to be launched to L2 in 2028. The proposed optical module of ATHENA consists of a single X-ray telescope with an effective area of about 1.4 m^2 at 1.0 keV and 0.25 m^2 at 6 keV, focal length of 12 m and angular resolution of 5 arcsec.

To realize such a large aperture X-ray telescope a technology, base on Silicon Pore Optics (SPO) was selected. SPOs were developed in ESTEC since 2004 and consist in the shaping of Silicon plates to the desired optical design. The realization of SPOs Mirror Modules (MMs) is appointed to Cosine B.V.[3] company. In summary, the manufacturing process consists in stacking of doubly-side polished silicon wafers, previously wedged and grooved. The adhesion of the plates is ensured by molecular Van der Waals interactions between the two silicon oxide

e-mail: giorgia.sironi@inaf.it, Telephone: +39-02-72320468

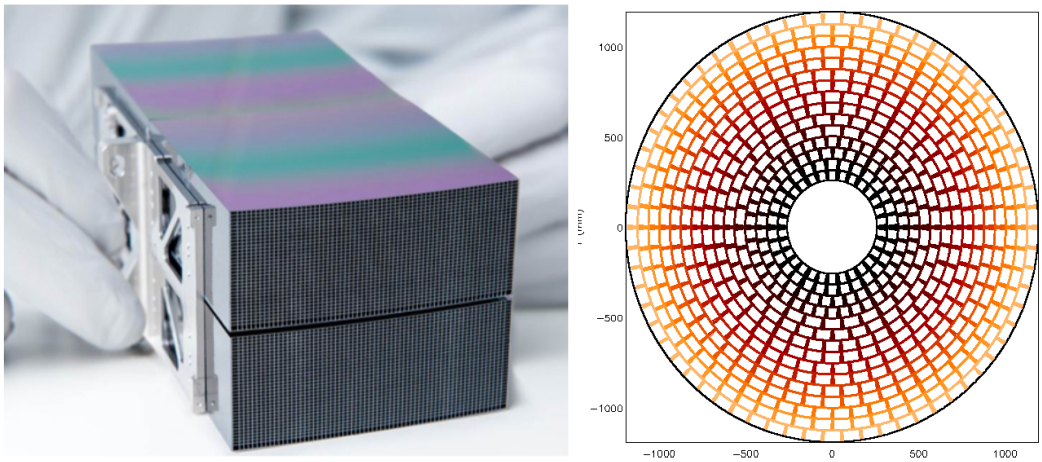

Figure 1. Left: A Wolter I SPOs mirror module (image credits ESA). The MM is realized as a double stack of 34 plates assembled in Wolter I configuration. Right: Graphic representation of the MMs positions in the ATHENA telescope. The MMs are organized in 15 rows with hexagonal symmetry.

surfaces, when they come into contact. The shaping of the plates is defined by the first layer assembled, formed on a silicon mandrel with either parabolic (primary) or hyperbolic (secondary) shape, reconstructing e.g., the widespread Wolter-I configuration.[2] Each MM is obtained[4] assembling the two shaped stacks, each composed by two sections of 34 layers: moreover, to simplify the final population of modules into the ATHENA optics structure, each MM includes two primary-secondary systems, operating in parallel. The typical height of a pore is of 0.606 mm and its width is 0.83 mm (Figure 1-left). Considering the silicon plates dimension and the process characteristics, the MMs dimensional feasibility limit was set at about 100 mm. This means that to populate the full telescope area a large number of MMs is required. In the configuration proposed by ESA (hereafter named configuration 3) the MMs are organized in 15 rows within six identical petals as in Figure 1-right, for a total of 678 units (Table 1).

The number of MMs to be produced is very large, but the SPOs technological solution offers great advantages for the realization of the optical module. They are:

- The replica process: just like nickel electroforming, the SPOs technology concentrates the efforts on the mandrel in order to improve the mirror quality. This means that time and costs for the shaping do not increase in proportion with the number of optical modules: they have to be allocated only once to produce the mandrel for each ring, instead of once a mirror like in the direct polishing technique. This solution has a strategic impact for mass production.
- The quality of the initial surfaces: as for the glass shaping, silicon plates are available on semiconductor markets at affordable costs with intrinsic low roughness. This avoids the iterative fabrication of super-polished optical surfaces required by direct polishing (for mirrors) and nickel electroforming (for mandrels).
- Physical characteristics of silicon: monocrystalline silicon has very high thermal conductivity, which makes it suitable to minimize the thermal gradients and the consequent thermal distortions.

The development of the SPOs technology also poses challenging aspects, which are being currently assessed:

- The approximation in the design: each plate in a MM does not come into contact with a mandrel with a designated shape when its shape is frozen into the stack: it is, rather replicated from the previous layer, with the addition of a wedge. Hence, that the optical surfaces be representing the desired focusing optical shape is not ensured. This approximation requires a considerable effort in the system simulation tool.

Table 1. ATHENA's configuration 3 parameters. MMs are organized on 15 rows with hexagonal symmetry. The radius of the central plate is reported below. The width of the MMs was defined considering the symmetry and the feasibility limit of the plates. The length of the MMs was defined to make each module self-baffling.

Row	#MM	Radius [m]	Width [mm]	Lenght [mm]
1	30	0.286	37.096	101.504
2	30	0.348	50.158	83.388
3	36	0.411	49.838	70.762
4	42	0.473	49.613	61.46
5	30	0.535	89.363	54.321
6	36	0.597	82.476	48.671
7	42	0.659	77.571	44.087
8	42	0.722	86.892	40.294
9	48	0.784	82.053	37.101
10	48	0.846	90.205	34.383
11	54	0.908	85.538	32.036
12	54	0.970	92.782	29.99
13	60	1.032	88.326	28.191
14	60	1.095	94.845	26.597
15	66	1.157	90.608	25.175

- The effects on reflecting coating: in the originally proposed design, the baseline for the MMs coating was Ir/B_4C bilayer,[5] chosen to optimize the effective area. Experimental tests of the coating performance performed at DTU Space have shown instability of the B_4C coating, and incompatibility with the industrial processes involved in the production of SPO mirror modules.[6] Silicon carbide (SiC) is recommended as replacement for B_4C. For the configuration 3 the proposed coating baseline is Ir/SiC.[5,6]
- The complex integration of the mirror assembly: considering the number of involved MMs, the misalignment contribution to be allocated in the error budget to the integration process should be carefully studied.
- The small size of pores: the pore structure generates a situation analogous to classical nested shell configuration, with reduced spacing in both directions (radial and azimuthal). This means that off-axis obstruction and stray-light modeling cannot be neglected. The pores are not small enough to cause relevant diffraction effects in X-rays, but in the UV light the diffraction contribution would be dominant. As UV optical benches are envisaged to perform the mirror module alignment in the assembly, the impact of aperture diffraction on the MMs alignment performances should be accurately assessed.

In this paper we discuss the latest results of a parallel set of studies, financed by ESA, to address the of the ATHENA optical module. SIMPOSiuM (SIMulation of Pore OpticS and Modeling) is a collaboration between the Brera Italian National Institute for Astrophysics (INAF-OAB) and the National Space Institute at the Technical University of Denmark (DTU Space) to develop a SW tools package to simulate the optical performances of ATHENA. Results from the collaboration were already presented in previous papers.[7,8] Here we report the latest results on the simulations of ATHENA configuration 3. ASPHEA (Alignment of Silicon Pore Optics for Height Energy Astrophysics) is a project led by Media Lario, involving INAF-OAB for what concerns the simulation of the co-focality of MMs aligned on a UV bench and prone to diffractive effect. Previous results of this project were reported in previous works.[7–9] Here we report the result obtained for the case of 2 MMs with alignment simulated by means of an X-ray test facility with source at finite distance, like PANTER.[10]

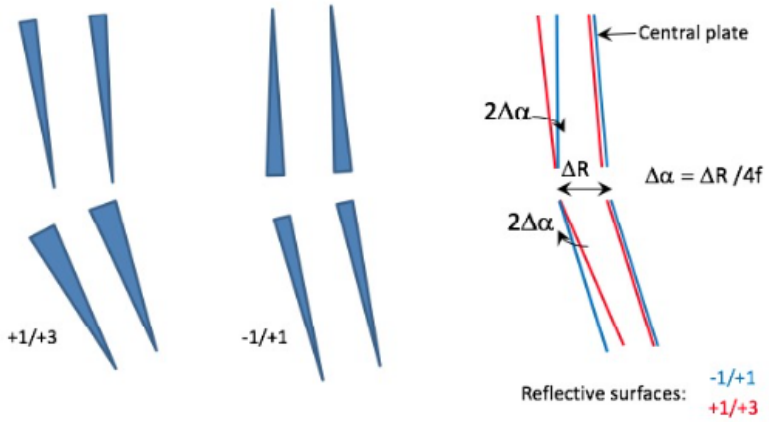

Figure 2. Different plate stacking in an SPO module, in radial section. Left: the +1/+3 wedge configuration requires manufacturing two different kinds of wedged plates. Center: the -1/+1 wedge configuration is obtained producing Silicon plates with the same wedge angle. Right: with respect to the +1/+3 wedge, the angle variation in the -1/+1 wedge configuration introduces an apparent source divergence $\delta n = 2n\Delta\alpha$ for the n-th plate, counted from the central one.

2. EFFECTIVE AREA SIMULATION

The effective area of ATHENA can be calculated by means of the IDL code presented in previous papers.[7,8] The code is based on the analytical computation of the illuminated area of each pore, extended to the full optical system. The code takes the following input information:

- *Wolter or Wolter-Schwarzschild design*: the intersection plane of different radially-distributed MMs can be considered at the same distance from the focal plane, along the axis or along the rays, respectively.
- *-1/+1 or +1/+3 wedge configuration*: in the Wolter I design, the incidence angle of the rays on the reflecting surfaces should increase by $\Delta\alpha = \Delta R/4f$ on the primary mirror one and by $3\Delta\alpha$ on the secondary one. To faithfully represent the Wolter I configuration, the primary stacks should have a wedge angle $\Delta\alpha$, while the secondary stacks should have a triple wedging (+1/+3). To simplify the manufacturing, however, a -1/+1 configuration was proposed. This solution foresees the only use of $\Delta\alpha$-wedged plates mounted in opposite directions to maintain the nominal angular difference between the two reflecting surfaces (Fig. 2). The decrease of effective area due to a +1/-1 wedge configuration is equivalent to a small off-axis effect, and was evaluated to be within 2%. Such value is acceptable, when compared to the relevant process simplification enabled by a single wedge manufacturing throughout the entire stack. We note that, even if each MM is composed by two primary+secondary parallel stacks, each individual stack has its central plate at the nominal angle. This was accounted for in the computation and contributed to reduce the effective area loss to the mentioned 2% level.
- *Variable filling factor (FF)*: ATHENA MMs are designed to be self-baffling. This means that the length of each MM is defined to make the maximum radius of a plate correspond to the inner radius of the next one (FF=1). This solution maximizes the effective area on-axis, but reduces the telescope field of view. In the case of SPOs technology, an approximation is intrinsic to the FF definition: the plates composing a MM have all the same length, but they are wedged to change the incidence angle, so it is possible to precisely assign the desired FF only to the central plate in each stack. Outer and inner plates would have FF<1 and FF>1, respectively.
- *Variable source off-axis angle*: the code allows to compute the effective area also for off-axis sources. The off-axis angle increases the obscuration of the pores and causes a major effective area decrease.

In Figure 3, top panel, we report the effective area computed for ATHENA's configuration 3 (Tab. 1). The effective area computation was performed for Wolter I design, -1/+1 wedging configuration and FF=1. The

computation was repeated for three cases of optimized reflecting coatings.[6] In Fig. 3, central and bottom panels we report the results of the same computation for the cases of a 10 arcmin and 20 arcmin off-axis source. The effective area values obtained at 1 keV and 6 keV are reported in Tab. 2 for reference.

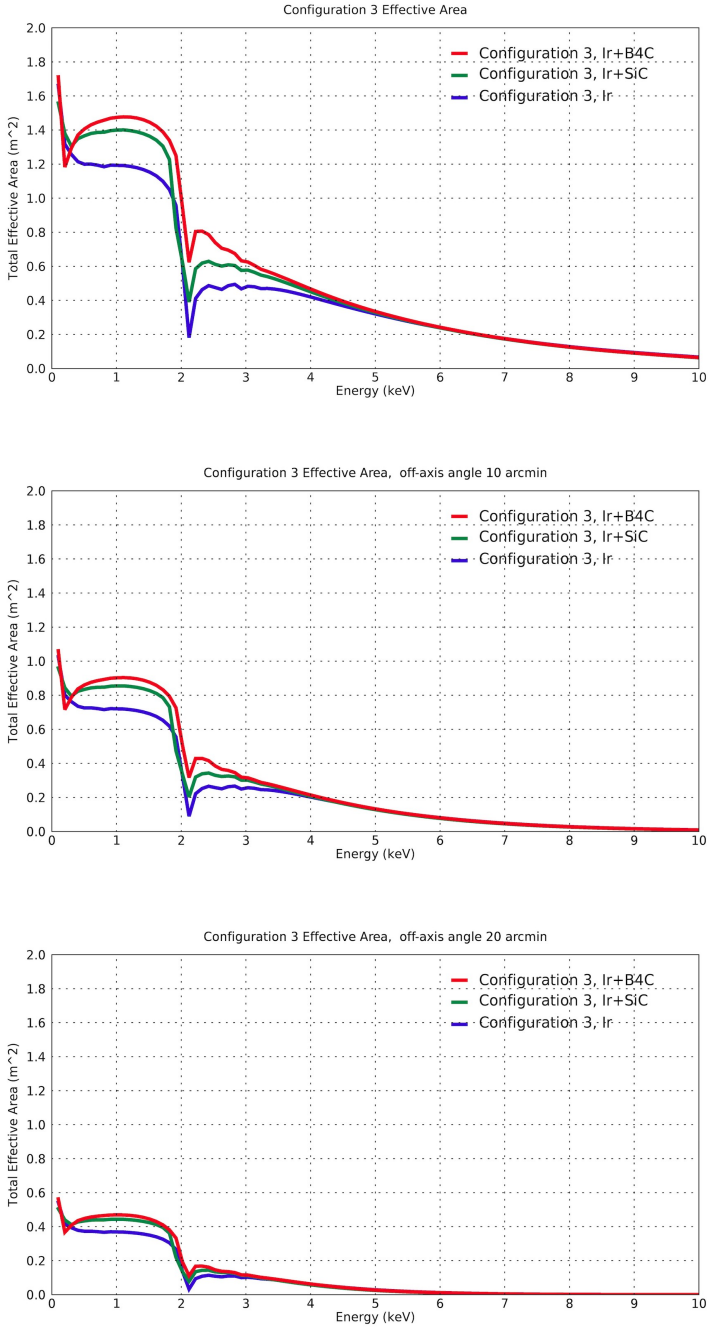

Figure 3. Energy-dependent Effective Area of ATHENA, configuration 3, as computed for three different coatings. The old configuration coating baseline Ir/B_4C (red curve), the new coating baseline Ir/SiC (green curve), and a plain Ir coating (blue curve) are shown. Top panel: results for an on-axis source. Central panel: results for a 10 arcmin off-axis source. Bottom panel: results for a 20 arcmin off-axis source

Table 2. Effective areas computed for ATHENA configuration 3 at 1 keV and 6 keV and for different off-axis angles.

	A_{eff}@1 keV $[m^2]$			A_{eff}@6 keV $[m^2]$		
Off-axis angle	0 arcmin	10 arcmin	20 arcmin	0 arcmin	10 arcmin	20 arcmin
Ir/B4C	1.474	0.902	0.469	0.242	0.080	0.011
Ir/SiC	1.399	0.854	0.443	0.238	0.077	0.010
Ir	1.193	0.720	0.369	0.238	0.081	0.012

3. OPTICAL SIMULATION USING MCXTRACE

Using an ATHENA-model setup with the ray tracing software package McXtrace, we may simulate various aspects of full-optic telescope performance. A simple way of doing this is to combine results from single mirror module simulations to obtain the performance of the entire optics.

Using McXtrace we trace rays through the mirror pores to ultimately land at the focal point. As rays enter the mirror module pores and get reflected by the mirror coating, we are able to follow the rays and assess stray light, on- and off-axis effective area, PSF, among other effects.

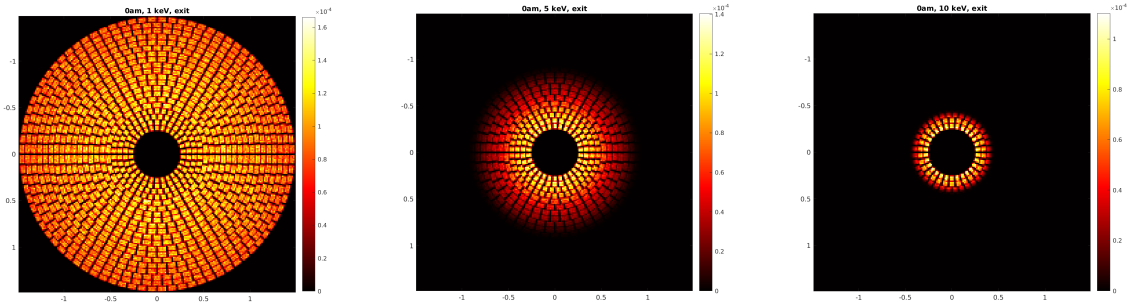

Figure 4. ATHENA optics through McXtrace ray-tracing. Example of simulated photons at exit of the optics for on-axis exposure with photon energies of 1 keV (left), 5 keV (center) and 10 keV (right).

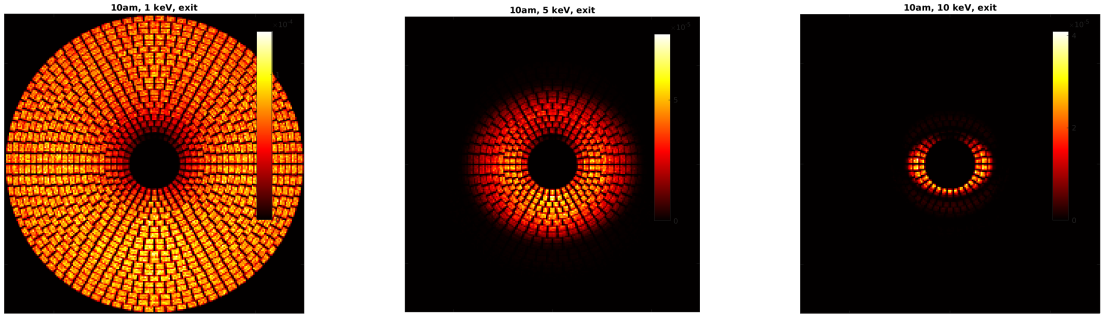

Figure 5. ATHENA optics through McXtrace ray-tracing. Example of simulated photons at exit of the optics for 10 arcmin off-axis exposure with photon energies of 1 keV (left), 5 keV (center) and 10 keV (right).

The energy dependence of the optics performance is also evaluated as low energies will be reflected throughout the entire optics, while higher energies will lose reflectivity for higher grazing incident on the outer mirror module rows.

Figure 4 shows the spatial intensity distribution just after the ATHENA-optic for 1 keV, 5 keV, and 10 keV respectively. Here it is clear how the low energy rays are reflected by all mirror modules in all mirror module rows and how as the X-ray energy increases, a smaller portion of the mirrors are able to reflect the traced rays.

In much the same manner we may evaluate off-axis performance. Instead of letting rays parallel to the optical axis impinge on the mirror modules, we may let the rays come from an arbitrary angle. We show an example of the off-axis simulation in Fig. 5 for the case of 10 arcmin off-axis angle around the horizontal axis. Also here, the energy dependence in the reflection of rays is evident, illustrating the kind of losses that can be expected as a function of X-ray energy and off-axis angle.

4. DIFFRACTION EFFECT OF MULTIPLE MIRROR MODULES

When SPOs technology is selected, a relevant contribution to the angular resolution error budget has to be allocated to MMs integration due to the large number of modules to be aligned. The geometrical misalignment of the MMs can be easily managed by McXtrace. However, the adoption of SPOs technology requires a deeper analysis of the diffraction effect due to the pore intrinsic high obstruction. This effect does not relevantly affect the X-ray angular resolution, which will be dominated by the plates shape errors, but it is quite strong in UV. Considering the case of the UV test facilities adopted for the MMs alignment during integration process, the simulation of diffractive effects is definitely relevant to ATHENA.

Usually, the effects of profile error and diffraction are faced with separate simulation tools: on one side, a geometrical ray-tracing is used to simulate the optical quality degradation due to surface shape error; on the other hand, the aperture diffraction can be simulated by means of Fresnel equations. The main problem in this approach is that the transition region between the two phenomena is extended, and a cut-off value of λ is impossible to set in general.[11]

A conclusive solution is to simulate the whole system by means of physical optics. The treatment of the diffraction of SPOs and the introduced approximations were already been discussed in a previous paper.[7] A direct comparison of the performed simulations with the experimental observed diffraction images was possible at Media Lario UV (218 nm) optical bench[9] and provided a successful validation of the method. Finally, also the invariance of the PSF centroids positions of X-ray and UV images, even at the presence of profiles longitudinal errors, was already presented one year ago.[8] That confirmed that an integration process based on UV illumination is well suitable for SPOs to achieve the requested alignment accuracy.

Here, we show that the adoption of a light source of finite dimensions, like the test facility ones, does not affect the alignment of two co-focal MMs. A simulation was performed modeling the Complex Pupil Function (CPF) of two flawless Wolter I MMs (Figure 6). The MMs where represented as two 42 mm illuminated regions separated by a dark equal dimension area. The radial distance of the mean plate of the MMs is 737 mm and the pore dimensions are 0.606 mm by 0.83 mm with with rib thickness of 0.17 mm. The variable shade of red represent the optical path distance variation through the layers, the distance obviously increases with radius. This simulation reproduces a real alignment test performed at PANTER.[9]

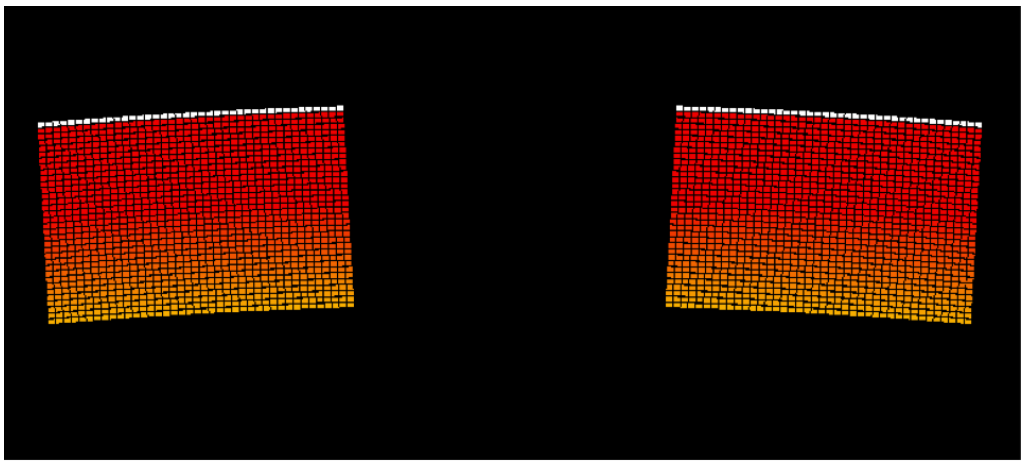

Figure 6. CPF model used to simulate the co-focality of two separated MMs. Two MMs are considered separated by a dark area, the variable shade of red represent the optical path distance variation through the layers.

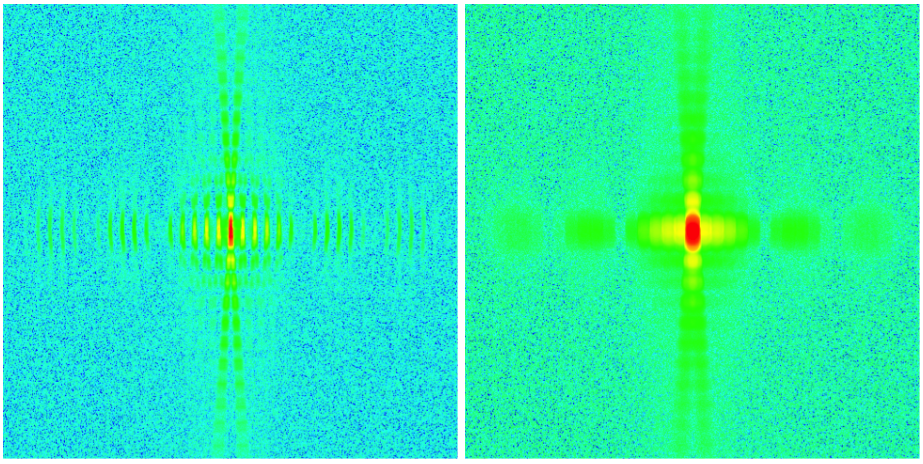

Figure 7. Best-focus configuration of two separated MMs, considered to have perfect Wolter I surfaces. The detector field is 2 mm and the pixel size is 1 μm. Left: PSF of two MMs illuminated by a 0.25 arcsec source. Right: PSF of two MMs illuminated by a 1 arcsec source.

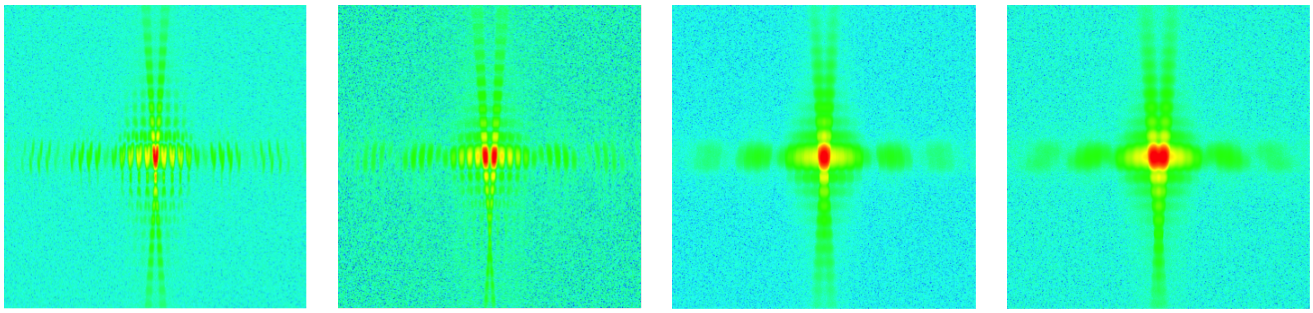

A) B) C) D)

Figure 8. The same configuration shown in Figure 7: moving a 2 mm wide detector intra-focal by A) 3 mm and B) 1 cm, considering a source 0.25 arcsec wide. Moving a 2 mm wide detector intra-focal by C) 3 mm and D) 1 cm, considering a source 1 arcsec wide.

The detector was simulated as a 2 mm wide area, with 2 μm spatial resolution. The best focus image was calculated at the distance foreseen for the finite distance light source case. In this case, the simulated test facility is the X-ray PANTER,[10] characterized by a source distance of 123.822 m. In this configuration the best focus for a MM with a focal length of 12 m results to be shifted by 1.288 m.

To understand how a realistic test could take place we simulated the PSFs moving the detector at intra-focal position, looking for a clear separation of the two foci. In Fig. 8A,B we reported the results obtained for the simulation of a 0.25 arcsec wide source and in Fig. 8C,D for an 1 arcsec wide source at the intra-focal positions of 3 mm and 1 cm. The separation between the two foci is clearly visible at 3 mm intra-focal when a small source size is used. Using a larger source, the separation becomes appreciable only defocusing the image by about 1 cm.

5. MAGNETIC DIVERTER FIELD SIMULATION

The background caused by soft protons (E $<$ 100 keV) is a major issue in X-ray telescope, and so is for ATHENA. To avoid the focalization of protons by the optics onto the focal plane instruments without affecting the X-ray flux, a well-known countermeasure is represented by a magnetic field with appropriate orientation and intensity. The magnetic field deviates the particles out of the detector area and so can keep the soft proton background to acceptable levels. In the case of ATHENA, the baseline solution adopted by ESA is represented by an Halbach array of permanent magnets in a pseudo-cylindrical geometry, so that the magnetic field is enhanced in the bore and cancelled outside. The magnetic field confinement, which is essential to avoid potential malfunction of the focal plane detectors, is obtained by a rotating orientation of magnetic dipoles in the array. This approximate

geometry can be easily obtained by assembling eight trapezoidal bars, forming a closed circuit. The methodology adopted to model a magnetic field generated by such an assembly of magnetic bars and wedges has been already detailed in a previous paper.[8]

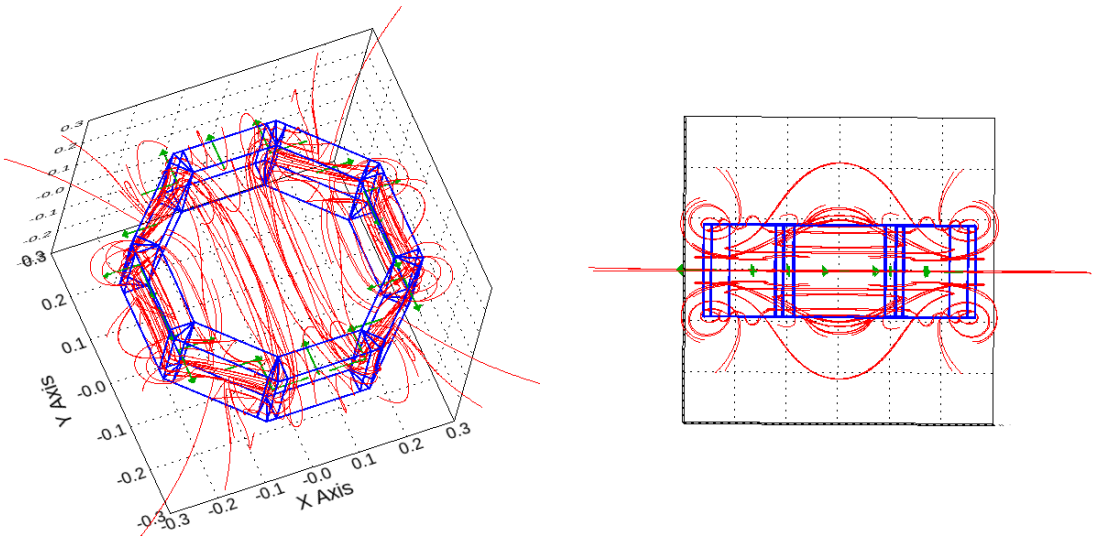

A) B)

Figure 9. Some simulated magnetic induction field lines, in the updated design of the Halbach array. A) Tilted view. B) Viewed sideways.

In this paper, we provide an updated sizing of the Halbach array with an enhanced magnetic field, in order to meet not only ATHENA's background specifications, but also the recent simulations on scattering of protons by SPO.[12] Assuming an ideal configuration with a constant field within the array bore and zero outside, computation shows that in order to deflect even the most laterally-directed proton, at the maximum energy (76 keV) that would make it –after the losses in the filters – fall on the WFI in its sensitivity range, the Halbach array should be 18 cm long and have a $\sim$ 500 G field within a 42.6 cm internal diameter bore. This value assumes the configuration 3 of the optics (Tab. 1), and 1 m space between the array and the focal plane. We also assume a magnetic dipole density of 1.1 T.

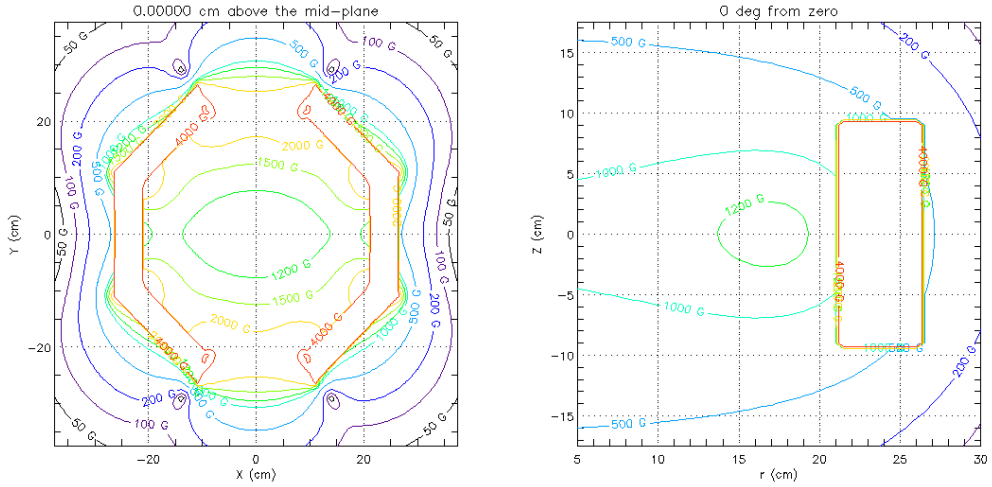

A) B)

Figure 10. Isocontours of the magnetic induction intensity. A) Median section of the array. B) Radial section. We easily see that the field is above 500 G within all the internal volume of the Halbach array.

With these assumptions, we could find that the needed level of magnetic field intensity within the bore can be reached easily with 5 cm thick magnets, and a total mass of the magnetic assembly is 106 kg (not accounting for the robust structure that will be necessary to safely keep the assembly in place). The magnetic induction intensity is mostly oriented along the y-axis (Fig. 9) and exceeds 500 G within all the bore (Fig. 10), while it decays rapidly outside it.

Future development of this work will include particle tracing through the simulated magnetic assembly, coupling the output of the SPO-particle interaction, as simulated by Geant4.[12] The particle tracing routine will allow us to determine the Halbach array efficiency at minimizing the proton background, assuming realistic values for the energy and the angular spread of the oncoming proton beam.

6. CONCLUSIONS

In the framework of the SIMPOSiuM project (financed by ESA), INAF-OAB and DTU Space developed a set of software tools to simulate ATHENA optics performances. The simulations cover both domains of geometric and physical optics. In this paper we reported the results obtained for the optical performance simulations of the new ATHENA design, with reduced maximum optics diameter and reflective coating change. We also report an updated of the results obtained for the ASPHEA project about the alignments of multiple MMs by means of real test facilities and a few simulations of the magnetic field achievable in a Halbach array, generating an effective magnetic field for proton deflection.

ACKNOWLEDGMENTS

The authors thank ESA for supporting this work with the contracts SIMPOSiuM (contract No. 4000114931) and ASPHEA (contract No. 4000111244).

REFERENCES

[1] Bavdaz, M., Wille, E., Shortt, B., et al., "The ATHENA optics development," Proc. SPIE 9905, 990527 (2016)

[2] Van Speybroeck, L.P., Chase, R. C., "Design parameters of paraboloid-hyperboloid telescopes for X-ray astronomy," Appl. Opt. 11(2), 440 (1972)

[3] Collon, M. J., Vacanti, G., Günther, R., et al., "Silicon pore optics for the ATHENA telescope," Proc. SPIE 9905, 990528 (2016)

[4] Collon, M., Vacanti, G., Barrière, N., et al., "Development of Athena mirror modules," Proc. SPIE 10399, 103990C (2017)

[5] Della Monica Ferreira, D., Massahi, S., Christensen, F. E., et al., "Design, development, and performance of x-ray mirror coatings for the ATHENA mission," Proc. SPIE 10399, 1039918 (2017)

[6] Della Monica Ferreira, D., Svendsen, S., Massahi, S. et al., "Performance and Stability of Mirror Coatings for the Athena Mission," Proc. SPIE 10699, 106993K (2018)

[7] Spiga, D., Christensen, F., Bavdaz, M., et al, "Simulation and modeling of silicon pore optics for the ATHENA X-ray telescope," Proc. SPIE 9905, 96055O (2016)

[8] Spiga, D., Della Monica Ferreira, D., Shortt, B., et al., "Optical simulations for design, alignment, and performance prediction of silicon pore optics for the ATHENA x-ray telescope," Proc. SPIE 10399, 103990H (2017)

[9] Valsecchi, G., Marioni, F., Bianucci, G., et al., "Optical integration of SPO mirror modules in the ATHENA telescope," Proc. SPIE 10399, 103990E (2017)

[10] Burwitz, V., Willingale, R., Pellilciari, C., et al., "Testing and calibrating the ATHENA optics at PANTER," SPIE Proc. 10399, 103990O (2017)

[11] Raimondi, L., Spiga, D., "Mirrors for X-ray telescopes: Fresnel diffraction-based computation of point spread functions from metrology," A&A 573, A22 (2015)

[12] Fioretti, V., Bulgarelli, A., Lotti, S., Macculi, C., et al., "The Geant4 mass model of the ATHENA Silicon Pore Optics and its effect on soft proton scattering," SPIE Proc., this volume (2018)